



**HAL**  
open science

## Experimental Determination and Representation of Binary and Ternary Diagrams of N-Hexacosane, N-Octacosane and N-Heptane

V. Ruffier-Meray, E. Behar, E. Provost, V. Chevallier, M. Bouroukba, M.  
Dirand

► **To cite this version:**

V. Ruffier-Meray, E. Behar, E. Provost, V. Chevallier, M. Bouroukba, et al.. Experimental Determination and Representation of Binary and Ternary Diagrams of N-Hexacosane, N-Octacosane and N-Heptane. *Revue de l'Institut Français du Pétrole*, 1998, 53 (1), pp.27-33. 10.2516/ogst:1998005 . hal-02078905

**HAL Id: hal-02078905**

**<https://ifp.hal.science/hal-02078905>**

Submitted on 25 Mar 2019

**HAL** is a multi-disciplinary open access archive for the deposit and dissemination of scientific research documents, whether they are published or not. The documents may come from teaching and research institutions in France or abroad, or from public or private research centers.

L'archive ouverte pluridisciplinaire **HAL**, est destinée au dépôt et à la diffusion de documents scientifiques de niveau recherche, publiés ou non, émanant des établissements d'enseignement et de recherche français ou étrangers, des laboratoires publics ou privés.



Distributed under a Creative Commons Attribution 4.0 International License

# EXPERIMENTAL DETERMINATION AND REPRESENTATION OF BINARY AND TERNARY DIAGRAMS OF *n*-HEXACOSANE, *n*-OCTACOSANE AND *n*-HEPTANE

**E. PROVOST, V. CHEVALLIER,  
M. BOUROUKBA and M. DIRAND**

Institut national polytechnique de Lorraine<sup>1</sup>

**V. RUFFIER-MERAY and E. BÉHAR**

Institut français du pétrole<sup>2</sup>

DÉTERMINATION EXPÉRIMENTALE  
ET REPRÉSENTATION DES DIAGRAMMES BINAIRES  
ET TERNAIRES DU *n*-HEXACOSANE, *n*-OCTACOSANE  
ET *n*-HEPTANE

L'accumulation des dépôts dans les conduites est un problème majeur lors de l'exploitation et du transport des bruts paraffiniques. La limitation de ces dépôts ou leur élimination par des méthodes telles que l'addition de produits chimiques, le raclage ou le réchauffage des conduites augmentent les coûts de production. Une meilleure connaissance du phénomène permettrait d'ajuster les schémas de production mis en œuvre et donc de limiter les coûts.

Des modèles thermodynamiques peuvent être utilisés pour calculer la température de cristallisation commençante et la quantité de dépôts solides en fonction de la température. Dans ces modèles, le fluide est représenté comme un mélange de corps purs ou de « pseudo-constituants » (qui représentent eux-mêmes plusieurs constituants purs). Pour décrire le comportement thermodynamique de ces mélanges, il est nécessaire d'avoir des données sur les constituants purs ainsi que sur leurs mélanges mais ces données sont rares dans la littérature lorsque l'on s'intéresse aux composés lourds.

Ce travail consiste en l'étude de mélanges de *n*-paraffines lourdes : le *n*-hexacosane (noté  $C_{26}$ ) et le *n*-octacosane (noté  $C_{28}$ ) dans le *n*-heptane (noté  $C_7$ ). Nous présentons ici la solubilité du  $C_{26}$ , du  $C_{28}$  et du mélange équimolaire de  $C_{26}$  et  $C_{28}$  dans le  $C_7$ , ainsi qu'une coupe isotherme ( $T = 303,15$  K) du diagramme ternaire. Les résultats expérimentaux sont restitués de façon satisfaisante par un calcul utilisant des expressions simples de l'énergie de Gibbs d'excès (NRTL et Redlich-Kister). Ce travail permet d'envisager la modélisation du comportement de systèmes complexes en utilisant uniquement des coefficients d'interaction binaires.

EXPERIMENTAL DETERMINATION AND  
REPRESENTATION OF BINARY AND TERNARY  
DIAGRAMS OF *n*-HEXACOSANE, *n*-OCTACOSANE  
AND *n*-HEPTANE

Accumulation of waxy deposits is a commonly occurring problem during exploitation and transportation of paraffinic crude oils. Limitation of these undesirable solids or removal by methods such as addition of chemical inhibitor, scrapping or heat tracing of flowlines, increase production costs. A better knowledge of this

(1) Laboratoire de thermodynamique des séparations,  
École nationale supérieure des industries chimiques,  
1, rue Grandville,  
54001 Nancy Cedex - France

(2) 1 et 4, avenue de Bois-Préau,  
92852 Rueil-Malmaison Cedex - France

phenomenon will make it possible to adjust process operating parameters and limit the operating costs.

Thermodynamic models can be used in order to calculate the wax appearance temperature and the amount of solid deposit versus temperature. In these models, the crude oil is represented as a mixture of pure or "pseudo-components" (which content several pure components). To describe the thermodynamic properties of those mixtures, data on pure components and on their mixtures are necessary but they are very scarce for heavy components in the literature. This work is devoted to the study of a mixture of heavy components including two heavy *n*-alkanes (*n*-hexacosane, denoted  $C_{26}$  and *n*-octacosane, denoted  $C_{28}$ ) and a solvent (*n*-heptane denoted  $C_7$ ).

Measurements of solubility of  $C_{26}$  and  $C_{28}$  and of equimolar mixture of  $C_{26}$  and  $C_{28}$  in  $C_7$ , and an isothermal ternary diagram of the mixture of the three components at 303 K are presented. Their calculations using simple expressions of Gibbs molar energy (NRTL and Redlich-Kister) are in good agreement with experimental data. The work allows to consider calculating complex systems with the only use of binary interaction coefficients.

#### DETERMINACIÓN EXPERIMENTAL Y REPRESENTACIÓN DE LOS DIAGRAMAS BINARIOS Y TERNARIOS DEL *n*-HEXACOSANO, *n*-OCTACOSANO Y *n*-HEPTANO

La acumulación de sedimentos en las canalizaciones constituye un importante problema durante la operación y el transporte de los crudos parafínicos. La limitación de estos sedimentos o sencillamente su eliminación, por aplicación de métodos, como, por ejemplo, la adición de productos químicos, el raspado o el calentamiento de las canalizaciones, vienen a aumentar los costes de producción. Así, un mejor conocimiento del fenómeno permitiría ajustar los esquemas de producción implementados y, por ende, limitar los costes.

Existe la posibilidad de utilizar modelos termodinámicos para calcular la temperatura de cristalización en su etapa inicial y el volumen de sedimentos sólidos en función de la temperatura. En estos modelos, el fluido está representado como una mezcla de cuerpos puros o de "seudocomponentes" (que representa a su vez varios componentes puros. Para describir el comportamiento termodinámico de estas mezclas, es preciso disponer de los datos acerca de los componentes puros, así como de sus mezclas, pero tales datos figuran en muy contados casos en la literatura profesional cuando se trata de conocer los componentes pesados.

Este trabajo consiste en estudiar las mezclas de *n*-parafinas pesadas a saber: el *n*-hexacosano (referencia  $C_{26}$ ) y el *n*-octacosano (referencia  $C_{28}$ ) en el *n*-heptano (referencia  $C_7$ ). Presentamos en este trabajo la solubilidad del  $C_{26}$ , del  $C_{28}$  y de la mezcla equimolar de  $C_{26}$  y  $C_{28}$ , en el  $C_7$ , así como una fracción isotermia ( $T = 303,15$  K) del diagrama ternario. Los resultados experimentales se restituyen de forma satisfactoria mediante un cálculo en que se utilizan expresiones simples de la energía de Gibbs de exceso (NRTL y Redlich-Kister). Este trabajo permite contemplar la modelización del comportamiento de sistemas complejos utilizando únicamente los coeficientes de interacción binarios.

## INTRODUCTION

Accumulation of waxy deposits is a commonly occurring problem during exploitation and transportation of paraffinic crude oils. Limitation of these undesirable solids or removal by methods such as addition of chemical inhibitor, scrapping or heat tracing of flowlines, increase production costs. A better knowledge of this phenomenon will make it possible to adjust process operating parameters and limit the operating costs. Thermodynamic models can be used in order to calculate the wax appearance temperature and the amount of solid deposit versus temperature. In these models, the fluid is represented as a mixture of pure or pseudo-components (which content several pure components). To describe the thermodynamic properties of those mixtures, data on pure components and on their mixtures are necessary but they are very scarce for heavy components in the literature. This work is devoted to the study of a mixture of heavy components including two heavy *n*-alkanes (*n*-hexacosane, denoted  $C_{26}$  and *n*-octacosane, denoted  $C_{28}$ ) and a solvent (*n*-heptane denoted  $C_7$ ). The assessment of the thermodynamic properties of such a mixture should increase the reliability of the calculations of complex systems.

## 1 EXPERIMENTS

### 1.1 Solubility

A simple thermal analysis device constructed in our laboratory was used to determine the solubility. A sample of known composition was introduced in an iron steel crucible. It was first heated until melting, and then slowly cooled. The actual measurement then began, by heating the sample at a temperature rate of 1 K/min. The apparatus was tested by measuring the melting temperature of the pure *n*-alkanes  $C_{26}$  and  $C_{28}$ . Results were in good agreement with those of the literature ( $\Delta T < 0.3$  K) [1] and [2].

### 1.2 Isothermal diagram

The following sequence was used to determine the isothermal diagram ( $C_{26}$ :  $C_{28}$ :  $C_7$ ) at  $T = 303.15$  K: the desired amount of  $C_{26}$ ,  $C_{28}$  and  $C_7$  was introduced in a syringe and melted. It was maintained in a thermostatic bath at a constant temperature ( $T = 303.15$  K) during at

least 1 hour, to ensure phase equilibrium. The liquid phase was picked through a filter ( $\varnothing$  0,45  $\mu$ m), and the remaining wet solid was dissolved in cyclohexane. Both solutions (containing the wet solid and the liquid) were analysed by gas chromatography. A mass balance, assuming that the solid is a binary mixture of  $C_{26}$  and  $C_{28}$ , and doesn't contain  $C_7$ , leads to the determination of the liquid and dry solid compositions.

## 2 RESULTS AND DISCUSSION

### 2.1 Binary systems

#### 2.1.1 Solubility

Measured solubility of  $C_{26}$  and  $C_{28}$  in  $C_7$  in a temperature range from 290 K to 350 K are shown in Figure 1, with those of Domanska [3] for the  $C_{28}$  in  $C_7$ . Our data are in good agreement with the literature values. As expected, the solubility of  $C_{26}$  is higher than that of  $C_{28}$ .

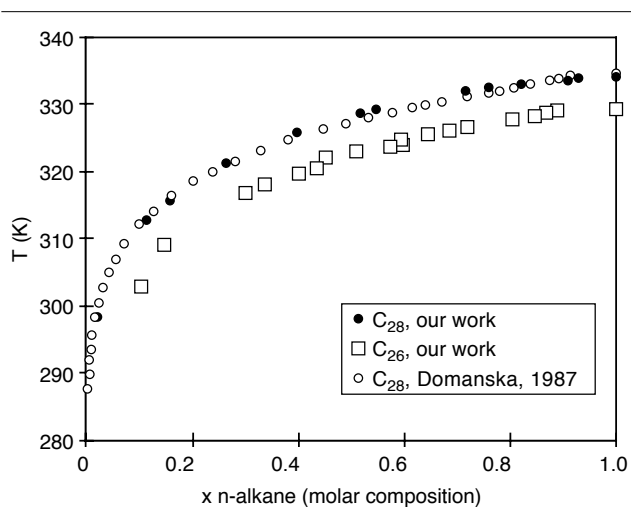


Figure 1  
Solubility of  $C_{26}$  and  $C_{28}$  in  $C_7$ . Experimental results and literature.

#### 2.1.2 Experimental activity coefficient

The activity coefficients  $\gamma$  of  $C_{26}$  and  $C_{28}$  have been calculated using the standard thermodynamic relationship for equilibrium between a pure solid component and a liquid:

$$\gamma = \frac{1}{x} \exp\left(-\frac{\Delta G(T)}{RT}\right)$$

where  $x$  is the molar composition of the liquid  
 $T$  is the equilibrium temperature  
 $\Delta G(T)$  is the melting Gibbs energy  
 $R$  is the universal gas constant  
 $= 8.31441 \text{ J}\cdot\text{mol}^{-1}\cdot\text{K}^{-1}$

$\Delta G(T)$  has been calculated in terms of enthalpy and entropy, leading to the following expression:

$$\begin{aligned} \Delta G(T) = & Cp^s \left[ T_{tr} - T \left( 1 + \ln \frac{T_{tr}}{T} \right) \right] \\ & + L_{tr} \left( 1 - \frac{T}{T_{tr}} \right) + Cp^{Rll} \left[ T_m - T_{tr} - T \ln \frac{T_m}{T_{tr}} \right] \\ & + L_m \left[ 1 - \frac{T}{T_m} \right] + Cp^{liq} \left[ T \left( 1 + \ln \frac{T_m}{T} \right) - T_m \right] \end{aligned}$$

In the above equation,  $T_m$  and  $L_m$  are respectively the temperature and the enthalpy of melting of the solid,  $T_{tr}$  and  $L_{tr}$  are the temperature and enthalpy of solid-solid transition,  $Cp^s$ ,  $Cp^{Rll}$  and  $Cp^{liq}$  the heat capacities of respectively the low temperature solid phase, the rotator phase and the liquid.  $Cp^s$  has been represented using Einstein's model [4].

The properties of the pure component ( $C_{26}$  or  $C_{28}$ ) were obtained from previous measurements [5], and are listed in Table 1.  $N$  and  $\theta$  are the Einstein's model parameters.

The evolution of the activity coefficient versus composition is represented in Figure 2.

TABLE 1

Thermodynamic properties of pure  $C_{26}$ ,  $C_{28}$  or in phase  $\beta''$

|          | $Cp^s$ |                | $Cp^{\beta''}$ |                | $Cp^{Rll}$<br>/J·mol <sup>-1</sup> ·K <sup>-1</sup> | $Cp^{liq}$<br>/J·mol <sup>-1</sup> ·K <sup>-1</sup> | $T_{tr}$<br>/K | $L_{tr}$<br>/kJ·mol <sup>-1</sup> | $T_m$<br>/K | $L_m$<br>/kJ·mol <sup>-1</sup> | $T_{\beta'' \rightarrow liq}$<br>/K | $L_{\beta'' \rightarrow liq}$<br>/kJ·mol <sup>-1</sup> |
|----------|--------|----------------|----------------|----------------|---|---|----------------|-----------------------------------|-------------|--------------------------------|-------------------------------------|--|
|          | N      | $\theta$<br>/K | N              | $\theta$<br>/K |   |   |                |                                   |             |                                |                                     |  |
| $C_{26}$ | 165.6  | 1553           | 194.5          | 1553           | 1363  | 850   | 325.9          | 32.9                              | 329.4       | 58.7                           | 327.0                               | 82.0   |
| $C_{28}$ | 161    | 1553           | 194.5          | 1553           | 1374  | 930   | 330.5          | 33.4                              | 333.9       | 61.9                           | 332.4                               | 88.0   |

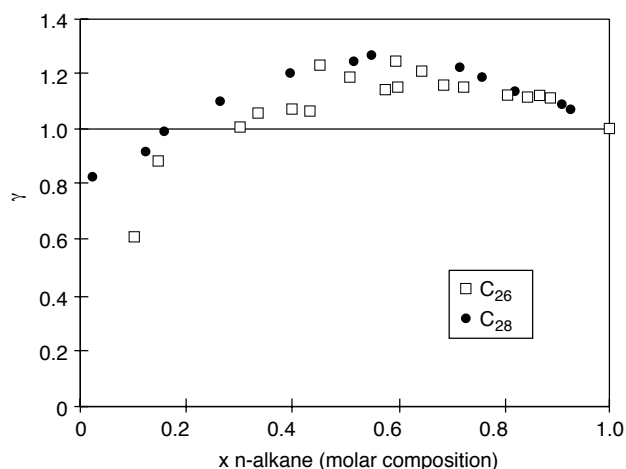


Figure 2

Activity coefficient of  $C_{26}$  and  $C_{28}$  in  $C_7$  versus molar composition.

It shows an atypical behaviour:  $\gamma > 1$  for low  $C_7$  composition, and  $\gamma < 1$  for higher  $C_7$  compositions. This phenomenon indicates a trend to association for high heavy *n*-alkane concentrations ( $C_{26}$  or  $C_{28}$ ) and to demixion for lower concentrations.

### 2.1.3 Calculated activity coefficients

The activity coefficient  $\gamma$  is related to the Gibbs molar partial excess energy by the well-known relation:

$$g_i^e = RT \ln \gamma_i$$

Two expressions of the Gibbs excess molar energy have been used [6] (NRTL and Margules):

$$\text{NRTL: } \frac{g^e}{RT} = x_{C_{26}} x_{C_{28}} \left( \frac{\tau_{21} G_{21}}{x_{C_{26}} + x_{C_{28}} G_{21}} + \frac{\tau_{12} G_{12}}{x_{C_{26}} G_{12} + x_{C_{28}}} \right)$$

$$\text{with } \tau_{12} = \frac{\Delta g_{12}}{RT}; \tau_{21} = \frac{\Delta g_{21}}{RT}$$

$$\text{and } \ln G_{12} = -\alpha \tau_{12}; \ln G_{21} = -\alpha \tau_{21} (\alpha = 0.4 [7])$$

the index 1 corresponds to  $C_{26}$  and the index 2 to  $C_{28}$ .

$$\text{Margules: } g^e = x_{C_{26}} x_{C_{28}} [A + B (x_{C_{26}} - x_{C_{28}})]$$

The parameters (reported in Table 2) have been fitted on the experimental curves of the activity coefficient  $\gamma$ .

TABLE 2

Parameters of the  $g^e$  equations

|                | Margules |      | NRTL            |                 |
|----------------|----------|------|-----------------|-----------------|
|                | A        | B    | $\Delta g_{ij}$ | $\Delta g_{ji}$ |
| $C_{26} + C_7$ | -154     | 1956 | 9978            | -3008           |
| $C_{28} + C_7$ | 650      | 1635 | 9749            | -2620           |

Both expressions lead to a good representation of the experimental solubility curves, as it can be seen in Figure 3, even if results are slightly better with NRTL. The mean temperature deviation  $\Delta T$  between calculated and experimental solubilities are given in Table 3.

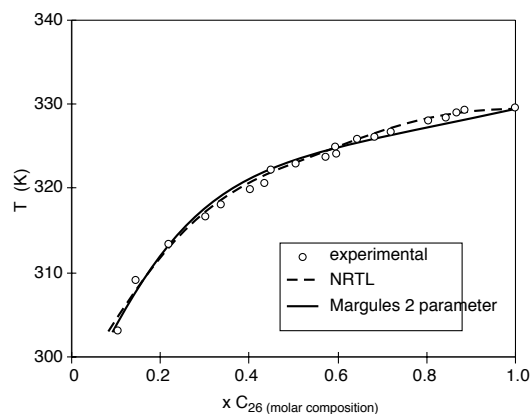


Figure 3

Solubility of  $C_{26}$  in  $C_7$ . Experimental and calculated results.

TABLE 3

Mean temperature deviation on the solubility results of  $C_{26}$  and  $C_{28}$  in  $C_7$

|                | Margules | NRTL |
|----------------|----------|------|
| $C_{26} + C_7$ | 0.70     | 0.46 |
| $C_{28} + C_7$ | 0.60     | 0.16 |

It is always lower than 0.7 K.  $\Delta T$  is calculated using the following expression:

$$\Delta T = \frac{1}{n} \sum_i^n |T_i^{\text{calc}} - T_i^{\text{exp}}|$$

with  $T_i^{\text{calc}}$  calculated temperature corresponding to the solubility point  $i$

$T_i^{\text{exp}}$  experimental temperature corresponding to the solubility point  $i$

$n$  number of experimental solubility points.

## 2.2 Ternary system

### 2.2.1 Results

Solubility of the equimolar mixture of  $C_{26}$  and  $C_{28}$  in  $C_7$  is presented in Figure 4. The isothermal diagram at  $T = 303.15$  K is presented in Figure 5.

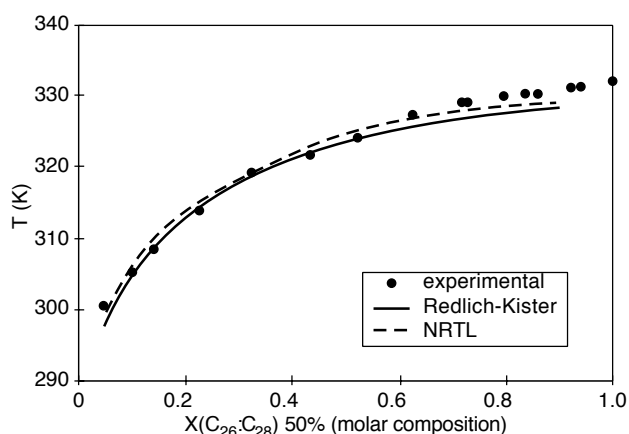


Figure 4  
Solubility of equimolar mixture of  $C_{26}$ :  $C_{28}$  in  $C_7$ . Experimental and calculated results.

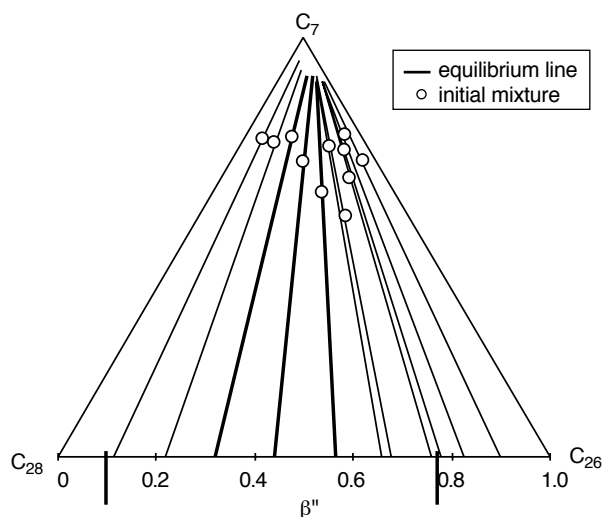


Figure 5  
Isothermal ternary diagram at  $T = 303.15$  K. Experimental results.

Additional X-ray diffraction measurements made on the solid phase in equilibrium with the ternary liquid mixture have showed that this solid has the same structure as the initial binary ( $C_{26}$ :  $C_{28}$ ) mixture.

Chromatographic results indicate that the solid is a binary mixture of  $C_{26}$  and  $C_{28}$ ; its composition is not the initial one [5]. Its structure is orthorhombic, denoted  $\beta''$ , distinct from the pure *n*-alkanes. This point will be taken into consideration in the diagram calculation. It is also observed that the solubility of  $C_{26}$  is higher when a small amount of  $C_{28}$  is added.

It is probably due to the formation of the orthorhombic intermediate solid phase  $\beta''$ , more soluble than the pure  $C_{26}$ : the structure of the  $\beta''$  phase presents a conformational disorder which increases the solubility of the solid.

### 2.2.2 Representation

Uniformity of the chemical potential in liquid and solid phases leads to the following system, allowing the calculation of the diagram:

$$\begin{cases} RT \ln \left( \frac{X_{C_{26}}}{x_{C_{26}}} \right) = \Delta G_{C_{26}}^{\beta'' \rightarrow liq.} (T) + g_{C_{26}}^{e, liq.} (x_{C_{26}}) - g_{C_{26}}^{e, \beta''} (X_{C_{26}}) \\ RT \ln \left( \frac{X_{C_{28}}}{x_{C_{28}}} \right) = \Delta G_{C_{28}}^{\beta'' \rightarrow liq.} (T) + g_{C_{28}}^{e, liq.} (x_{C_{28}}) - g_{C_{28}}^{e, \beta''} (X_{C_{28}}) \end{cases}$$

with  $x_i$  composition of the liquid phase

$X_i$  composition of the solid phase

$\Delta G_i^{\beta'' \rightarrow liq.} (T)$  Gibbs energy of melting of  $i$  from the solid  $\beta''$  to the liquid

$g_i^{e, liq.}$  Gibbs excess molar partial energy of  $i$  in the liquid

$g_i^{e, \beta''}$  Gibbs excess molar partial energy of  $i$  in the solid  $\beta''$ .

$\Delta G_i^{\beta'' \rightarrow liq.} (T)$  is calculated for each pure *n*-alkane, with the following expression:

$$\begin{aligned} \Delta G_i^{\beta'' \rightarrow liq.} (T) = & C_p^{\beta''} \left[ T_{\beta'' \rightarrow liq.} - T \left( 1 + \ln \frac{T_{\beta'' \rightarrow liq.}}{T} \right) \right] \\ & + L_{\beta'' \rightarrow liq.} \left[ 1 - \frac{T}{T_{\beta'' \rightarrow liq.}} \right] \\ & + C_p^{liq.} \left[ T \left( 1 + \ln \frac{T_{\beta'' \rightarrow liq.}}{T} \right) - T_{\beta'' \rightarrow liq.} \right] \end{aligned}$$



$T_{\beta'' \rightarrow \text{liq.}}$  and  $L_{\beta'' \rightarrow \text{liq.}}$  are the hypothetical temperature and heat of transition from the solid  $\beta''$  to the liquid,  $C_p^{\beta''}$  is the heat capacity of the phase  $\beta''$ . Values have been determined from thermodynamical measurements [5], and are reported in Table 1.

Different expressions of the Gibbs excess energy ( $g^e$ ) have been used to represent the liquid phase or the solid phase:

- Solid phase (binary mixture of  $C_{26}$  and  $C_{28}$ ):  
a two parameters Margules expression has been used. The parameters ( $A$  and  $B$ ) have been determined from the study of the binary diagram ( $C_{26}$ :  $C_{28}$ ) [5].

$$g^e = X_{C_{26}} X_{C_{28}} \left[ A + B (X_{C_{26}} - X_{C_{28}}) \right]$$

- Liquid phase (ternary mixture of  $C_{26}$ ,  $C_{28}$  and  $C_7$ ):  
two models have been used, NRTL and Redlich-Kister which is equivalent to Margules when applied to multicomponent systems, with the following assumptions:

- the mixture of  $C_{26}$  and  $C_{28}$  in the liquid state is an ideal solution ( $g^e = 0$ ). This point has been verified by Achour [8], for the binary system  $C_{26}$ :  $C_{24}$ ;
- ternary interactions are neglected.

The  $g^e$  equations are finally:

$$\text{NRTL: } \frac{g^e}{RT} = \sum_{i=1}^3 x_i \frac{\sum_{j=1}^3 \tau_{ji} G_{ji} x_j}{\sum_{k=1}^3 G_{ki} x_k}$$

with  $\Delta g_{23} = \Delta g_{32} = 0$  and  $\alpha = 0.4$

Redlich-Kister:

$$g^e = x_1 x_2 [A_{12} + B_{12} (x_1 - x_2)] \\ + x_2 x_3 [A_{23} + B_{23} (x_2 - x_3)] \\ + x_3 x_1 [A_{31} + B_{31} (x_3 - x_1)]$$

In these equations,  $i = 1$  for  $C_{26}$ ,  $i = 2$  for  $C_{28}$  and  $i = 3$  for  $C_7$ .

The calculation leads to a good representation of both solubility curves and the isothermal diagram; the calculated solubility of binary mixtures of  $C_{26}$  and  $C_{28}$  in  $C_7$  is presented in Figure 4 together with experimental points. Table 4 shows the mean percentage deviation  $\Delta x(\%)$  between experimental and

calculated compositions of the liquid phase (isothermal diagram).  $\Delta x(\%)$  has been calculated using the following expression:

$$\Delta x(\%) = \frac{1}{n} \sum_i^n \frac{|x_i^{\text{calc.}} - x_i^{\text{exp.}}|}{x_i^{\text{exp.}}} \times 100$$

with  $x_i^{\text{calc.}}$  calculated liquid phase molar composition

$x_i^{\text{exp.}}$  experimental liquid phase molar composition

$n$  number of experimental points.

In all cases, results are satisfactory. The hypothesis of negligible ternary interactions seems to be valid.

TABLE 4

Mean percentage deviation between experimental and calculated liquid phase of the isothermal ternary diagram (T = 303.15 K)

|          | Redlich-Kister | NRTL |
|----------|----------------|------|
| $C_7$    | 1.8%           | 0.6% |
| $C_{26}$ | 20.8%          | 7.2% |
| $C_{28}$ | 11.8%          | 5.9% |

## CONCLUSION

The solubility curves of  $C_{26}$ ,  $C_{28}$  and mixtures of  $C_{26}$  and  $C_{28}$  have been determined in *n*-heptane, as well as an isothermal diagram of the 3 components. Experimental results have been represented using simple expressions of the Gibbs excess energy (NRTL and Margules). The ternary system (solubilities and isothermal diagram) has been calculated from binary solubility parameters, taking into consideration the formation of an intermediate solid phase between  $C_{26}$  and  $C_{28}$ . Ternary interactions have been neglected. Results are good, for both solubilities and the isothermal diagram.

This work allows to consider calculating complex systems with the only use of binary interaction coefficients.

## ACKNOWLEDGEMENTS

The authors wish to thank the *Institut français du pétrole* for its financial support.

## REFERENCES

- 1 Andon R.J.L. and Martin J.F. (1976) Thermodynamic properties of hexacosane. *J. Chem. Thermodyn.*, 8, 1159.
- 2 Domanska U. and Wyrzykowska D. (1991) Enthalpies of fusion and solid-solid transition of even-numbered paraffins  $C_{22}H_{46}$ ,  $C_{24}H_{50}$ ,  $C_{26}H_{54}$  and  $C_{28}H_{58}$ . *Thermochim. Acta*, 179, 265.
- 3 Domanska U. (1987) *Inter. Data Ser., Selected Data Mixtures, Ser. A*, 4, 269.
- 4 Achour Z., Bouroukba M., Balesdent D., Provost E. and Dirand M. (1997) Variation in enthalpy of the system *n*-tetracosane: *n*-hexacosane as functions of temperature and composition. *J. Therm. Anal.*, in press.
- 5 Provost E. (1997) Thermodynamic and structural studies of two heavy *n*-alkanes (*n*-hexacosane and *n*-octacosane) and their mixtures in organic solvents containing seven atoms of carbon. *Ph.D.* Institut national polytechnique de Lorraine, Nancy, France.
- 6 Reid R.C. and Sherwood T.K. (1958) *The Properties of Gases and Liquids*, Ed. Mc Graw Hill, N Y.
- 7 Domanska U. and Rolinska J. (1989) Correlation of the solubility of even-numbered paraffins  $nC_{20}H_{46}$ ,  $nC_{24}H_{50}$ ,  $nC_{26}H_{54}$  and  $C_{28}H_{58}$  in pure hydrocarbons. *Fluid Phase Equilib.*, 45, 25.
- 8 Achour Z. (1994) Thermodynamic and structural study of *n*-tetracosane: *n*-hexacosane system. *Ph.D.* Institut national polytechnique de Lorraine, Nancy, France.

*Final manuscript received in December 1997*